2.2.2 *Human posture and activity monitoring*

The importance of ambulatory activity monitoring is well recognized in the fields of gerontology, rehabilitation, and general healthcare. In the field of gerontology, for example, one of the key aims in the care of the elderly is to maintain their daily activities at an appropriately high level and to particularly prevent their becoming bedridden.[32] In the rehabilitation field, a therapist must evaluate motion characteristics during standing up and walking among others; however, it is very much a situation in which he/she must usually make assessments subjectively by direct observation. Therefore, the quantitative assessment of activities is highly desirable. One method employed is to record using a three-dimensional motion capture system, but the range over which such recording is possible is usually limited and data analysis is complicated, rendering this system unsuitable for use in practical rehabilitation.

Some wearable instruments capable of monitoring activities using an accelerometer, a gyrosensor and so on have been developed.[33–38] Such wearable systems have not yet become practical in the rehabilitation field owing mainly to awkward and unsuitable means for the physically challenged or the elderly. With the aim of improving the quality of life for these persons, we have developed a portable and handy device for monitoring postural changes and activities by measuring the trunk, thigh, and calf angles with respect to the gravitational direction.[25–28] This device has recently been improved to make it more convenient for rehabilitation training as well as for collecting a daily record of activity scenarios.[8]

The principle of the measurement of posture together with walking speed is quite simple, as shown respectively in the left and the right panels of Fig. 6. If we can measure the angles of three anatomical parts, such as the trunk, thigh, and calf, with respect to the gravitational direction, we can discriminate almost all the human postures in the sagittal plane, which are possible under normal daily life. Using the thigh (θ_{21} and θ_{22}) and calf angles (θ_{31} and θ_{32}) at 'heel contact' and 'off' together with the subject's thigh (L_1) and calf length (L_2), the length of one stride (D_e) can be calculated using the two-link gait model. Therefore, the walking speed (V_e) for one walking cycle can also be calculated from D_e divided by the time of one step (T_e). The accuracy of the walking speed thus obtained has been shown to be highly precise over a wide range from 0.5 m/s or less (relatively slow pace of physically challenged or elderly people) to 2.0 m/s or more (considerably quick pace of healthy subjects) as compared with a video camera system.[27,28]

In Fig. 7, an overview of the wearable sensor system is shown. The accelerometer, gyrosensor, amplifier, micro-SD card, transmitter, battery, CPU, and other parts are installed in each of the sensor units, and the units are attached onto the subject's trunk, thigh, and calf. The subject's motion when in the medical center is monitored in real time using a telemetering system such as a W-BAN, and the activity data collected during normal daily living is saved on the micro-SD card.

The system can discriminate among postures, from walking, sitting, lying down, standing up, sitting down, and standing on the basis of the angle changes in the sagittal plane calculated from the low-frequency signals (DC, 0.5 Hz) of the accelerometers attached to each part. In the static postures of standing, sitting, and lying down, the angle

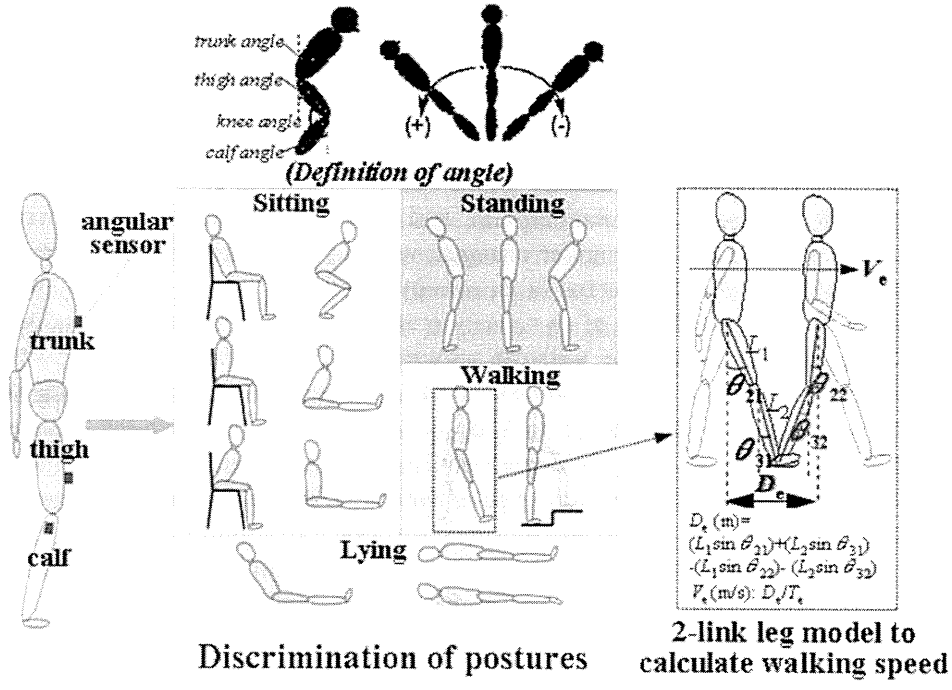

Fig. 6. Principles of determination of posture in sagittal plane by measuring trunk, thigh and calf angles with respect to gravitational direction (left panel), and walking speed for two-link leg model (right panel). The uppermost part shows the definition of angle for each anatomical segment. See text for explanation.

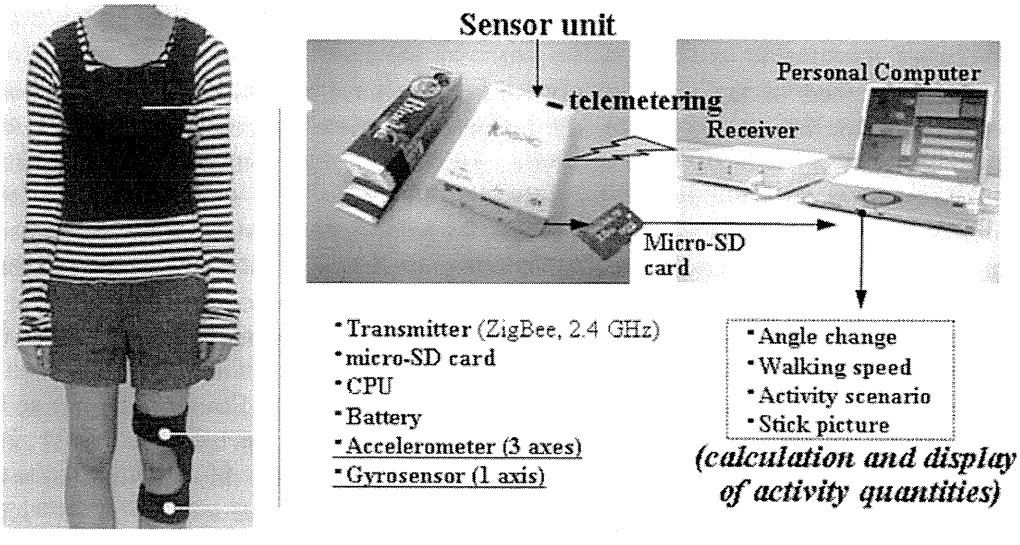

Fig. 7. Overview of wearable sensor system: Photos of user wearing sensor units in jacket pocket and knee support (left part), sensor unit (middle), and receiver together with personal computer (right).

of each part with respect to the gravitational direction is obtained from the low-frequency signals from the accelerometers. Additionally, to calculate the angular changes in the trunk, thigh, and calf during dynamic situations such as walking, the angular velocity outputs of the gyrosensors attached to each part are integrated. The initial angle is obtained from the accelerometer signal immediately before walking.

From the angular changes, activity scenarios are displayed as color bars (standing, walking, sitting, lying down, standing up, and sitting down) using the conventional personal computer. Detailed angular changes, walking speed, and motion pictures can also be displayed by clicking the bar of an activity scenario.

Figure 8 shows typical data of an activity scenario, thigh angle changes and walking speed during each walking cycle, with the associated stick pictures during six postures in a female subject with hemiplegia (84 yrs). It is clearly observed that although the subject was mostly living in either sitting or lying position, the cyclic angular changes and stable increase and decrease in walking speed can be detected during walking. The stick pictures derived from the angular changes of the trunk, thigh, and calf can also provide useful details of posture.

To investigate the system's applicability to patient activity monitoring in rehabilitation programs, we have successfully carried out clinical studies at some rehabilitation centers.[8,27,28] Through experiments in various situations including those in daily life, the system has been found to be promising for the quantitative evaluation of the efficacy of rehabilitation programs as well as human daily activities. As a future prospect, it is moreover desirable to obtain motion information with six degrees of freedom, and this will be realized by the use of a triaxial gyrosensor into the sensor unit.

3. Nonconscious Healthcare Monitoring at Home

As mentioned in the Introduction section, we have recently developed a home healthcare monitoring system on the basis of the new concept of "nonconscious physiological monitoring." This involves a procedure carried out in a fully automated manner without the attachment of any biological sensors to a subject's body or any troublesome operations of measurement. To achieve such monitoring, all sensors and instruments are built into home facilities, such as the toilet, bathtub, and bed, which are used in normal daily life. Thus, the subject does not need to be aware of the measurement being made, and the physiological data collected and stored are truly representative of ordinary daily living.

The daily use of the toilet by the subjects provides convenient opportunities for monitoring. We have developed a body and excretion weight monitor based on a highly accurate weighing scale device installed in the lavatory floor around the toilet bowl. Also, we have installed a BP monitoring system into the toilet seat.[7,14,15] For monitoring cardiac pulse and respiration, we have used vinyl tubes filled with silicone oil under a pillow.[16] For the care of the elderly, there is an important need for a drowning alarm in the bathtub, and we have designed a bathtub monitoring system capable of simultaneously detecting ECG together with respiration in the bathtub.[17]

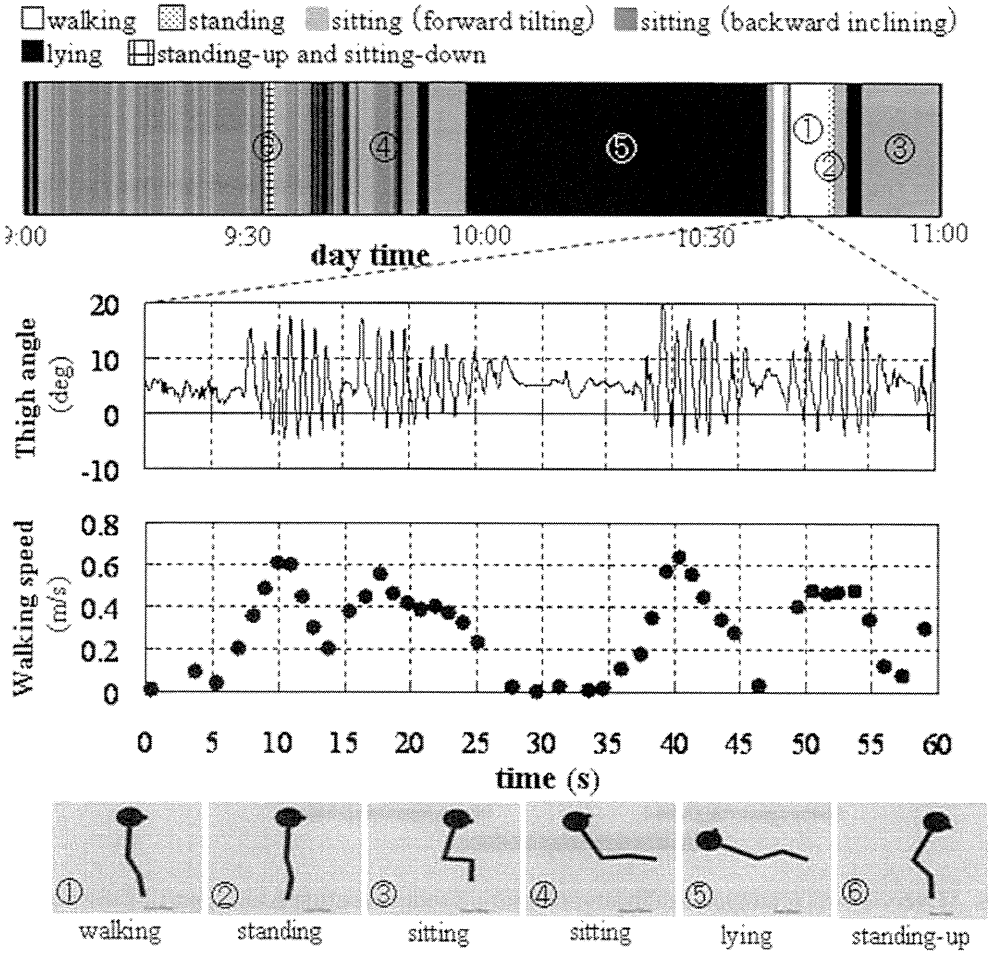

Fig. 8. Typical recordings obtained from a female subject with hemiplegia (84 yrs), showing activity scenarios from 9:00 to 11:00 a.m. (top panel), thigh angle change and walking speed during each walking cycle for a period of 60 s indicated by two dashed lines (middle part), and postural stick pictures (lowest panel), the numbers in which correspond to those in the scenario record. Various activities are indicated in the upper part of the scenario record.

To realize the whole concept, we have developed a new prototype healthcare monitoring room in which the systems for bathtub, toilet, and under-pillow monitoring are installed. We have evaluated the measurement accuracy and validity of these devices by simultaneous recordings of standard biological sensors directly attached to the subjects' body surface, and the results indicate that the new monitors do indeed allow accurate and reliable measurements.[7,14–17]

Figure 9 shows an overview of the prototype healthcare monitoring room, which has been constructed in a part of our laboratory in Kanazawa University. All the sensors and instruments are installed in the toilet space, the bathtub, and the bed. The obtained

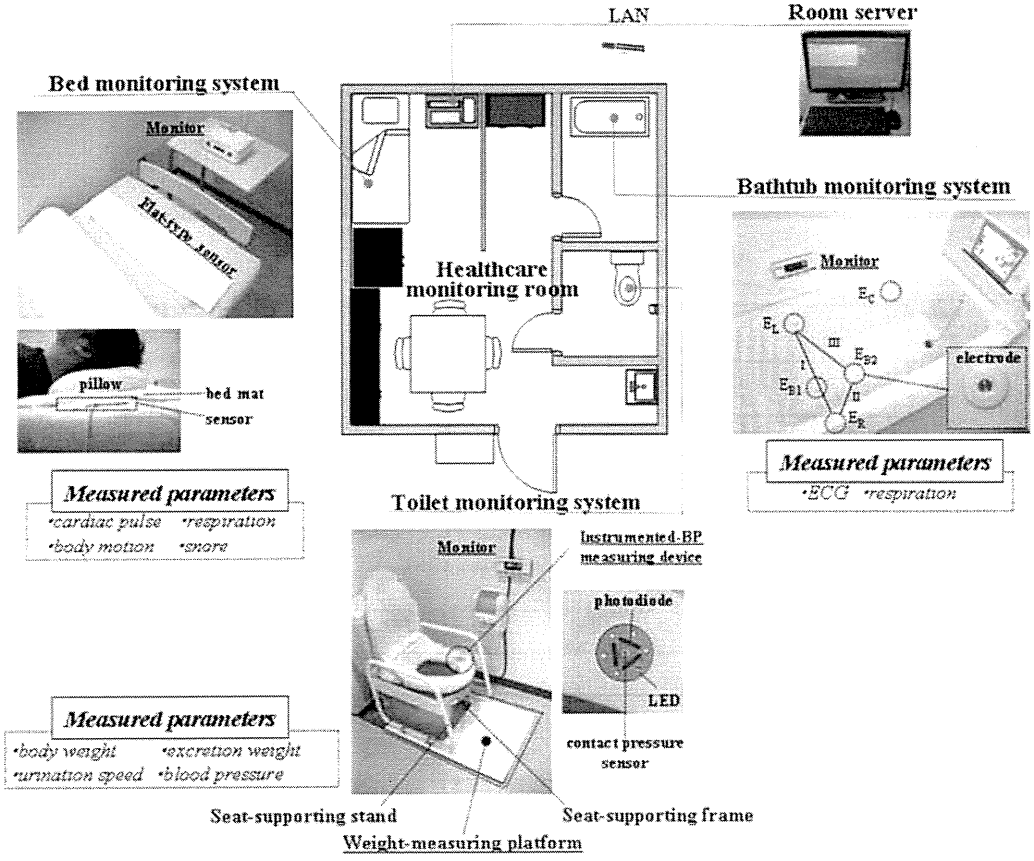

Fig. 9. Overview of prototype healthcare monitoring room constructed in a part of the author's laboratory in Kanazawa University. All the sensors and instruments are installed in the toilet space, bathtub, and bed. Measured parameters are shown for each system.

data are automatically analyzed and displayed using a monitoring system equipped with amplifiers for the sensors, a computer, memory, an LCD, and a LAN module. Analytical results from each sensor are stored and displayed using the room server.

In the toilet space, a platform-type scale with a weighing resolution of 5 grams is placed around the toilet bowl and is arranged to support the toilet seat using a frame. With this arrangement, the scale can accurately detect the total body weight before and after excretion, thereby obtaining excreta weight by subtracting body weight.

BP measurement is achieved using the volume-oscillometric principle, previously proposed by us.[7,20,21,23,39] A pusher plate is installed in the toilet seat, which applies local pressure against the back of one thigh pushed up by a pantagraph mechanism. The photoplethysmogram in the perforating arteries of the thigh is measured using six high-luminance near-infrared LEDs and three high-sensitive photodiodes affixed to the plate, which also houses a contact pressure sensor for measuring the pressure applied to the back of the thigh.

In the bed, a flat sensor (800×15×8 mm^3) is fixed under a pillow or a bed mat. It comprises four vinyl tubes filled with silicone oil sandwiched by two acrylic plates,[17] the width of which is aligned along a bed side. One end of each tube is connected to a pressure sensor and the other end is closed. The inner pressure in each tube changes in accordance with respiration, cardiac beating, and snoring, and each component can be detected using an appropriate digital filter. Moreover, periods of apnea and hypopnea can be detected from the decrease in amplitude of the respiration signal for more than 10 s, which is based on the definition of sleep apnea syndrome (SAS), using a fully automated analytical program. The DC level of the pressure output can provide information on whether the subject is lying on the bed.

For ECG monitoring in the bath, four stainless steel electrodes are fixed to the inner wall of the bathtub essentially surrounding the subject's chest, so as to place them in the standard Einthoven's triangle configuration. One of the four electrodes is used as the reference electrode placed far from the other three electrodes. The potential differences between two electrodes, similar to the conventional lead-I, lead-II, and lead-III, are amplified to obtain a raw ECG signal. This signal contains a baseline fluctuation due to respiration, and thus, can be filtered with a digital filter, obtaining a clear ECG and a respiration component.[12] The fluctuations of R-R intervals in accordance with respiratory sinus arrhythmia are also used for the detection of the respiratory component.[17]

Figure 10 shows examples of recordings of the changes in body weight during urination (a) and those in BP measurement (b) using the toilet-installed monitoring system in a healthy male subject (25 yrs). Usually, after standing on the platform or sitting on the toilet seat, very large artifact signals due to body movements are observed immediately before and after urination (or defecation). These components are reduced due to less motion during urination (or defecation); therefore, the system can detect the body weights at the start and end of excretion, and thus, excretion weight can be obtained from the difference between the two body weights. Furthermore, the other components, i.e., ballistocardiogram (BCG) in association with cardiac beats, are observed superimposed on the weight change signal, as shown in Fig. 10(a). The rate of urination is obtained from the weight change signal smoothed by an appropriate filter, obtaining urination flow rate.

It is also noted that the initial phase of a BCG signal originates from the ejecting blood flow from the ventricle,[40,41] i.e., differentiation of the ventricular volume change. Therefore, stroke volume (SV) and thus cardiac output (CO = SVx (heart rate)) could be estimated from BCG signals together with BP as obtained below.[41]

In Fig. 10(b), the simultaneously obtained records of the pulsatile component of the photoplethysmogram (PGac) are shown with the applied contact pressure for BP measurement. The pressure measurement reference is compensated for the subject's heart level by the hydrostatic pressure difference between the measuring site and the heart. According to the volume-oscillometric method,[39] the systolic (SBP) and the mean BP (MBP) can be indirectly determined from the applied pressure corresponding respectively to the systolic end point and the maximum amplitude point of PGac.

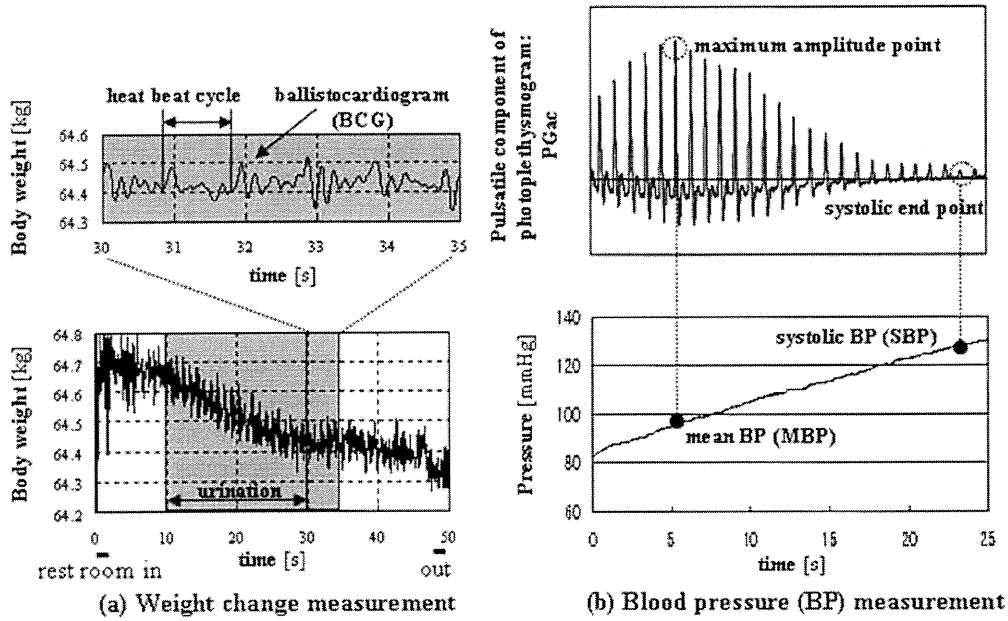

Fig. 10 Example of recordings using the toilet-installed monitoring system obtained from a healthy male subject (25 yrs). In (a), the signals for body weight (BW) change following urination and the ballistocardiogram (BCG) superimposed on the BW signals (upper part) are shown. (b) shows the simultaneous records of the pulsatile component of the photoplethysmogram (PGac) and the applied contact pressure for the measurement of blood pressure (BP). By the volume-oscillometric method, systolic (SBP) and mean BP (MBP) can be indirectly determined from applied pressure corresponding respectively to the systolic end point and the maximum amplitude point of PGac.

The upper two records in Fig. 11 show an example of respiration signals obtained by the bathtub electrodes (upper panel) and a chest band (lower panel) before and immediately after simulated drowning with the head bent forward in a healthy male subject (24 yrs). In the lower two records are shown ECG signals obtained by the bathtub electrodes (upper panel) and ECG electrodes directly attached to the subject's body surface (lower panel) during a part of drowning indicated by a shadow in the upper records. It is clearly observed that the respiration and ECG signals detected by the two methods agree well with each other, and that the ECG signals continue to be observed but no respiration signals can be obtained during the simulated drowning.

In the upper two records of Fig. 12 are shown respiration signals using the under-pillow sensor (upper panel) and a respiration chest band (lower panel) before and immediately after a period of simulated apnea obtained in a healthy male subject (25 yrs) in the supine position. The lower two records, which are the shadow part in the upper records of Fig. 12, show the cardiac pulse signal obtained by the under-pillow sensor (upper panel) and the ECG signal detected from the ECG electrodes directly attached to the body surface (lower panel). From these results, it is demonstrated that the respiration

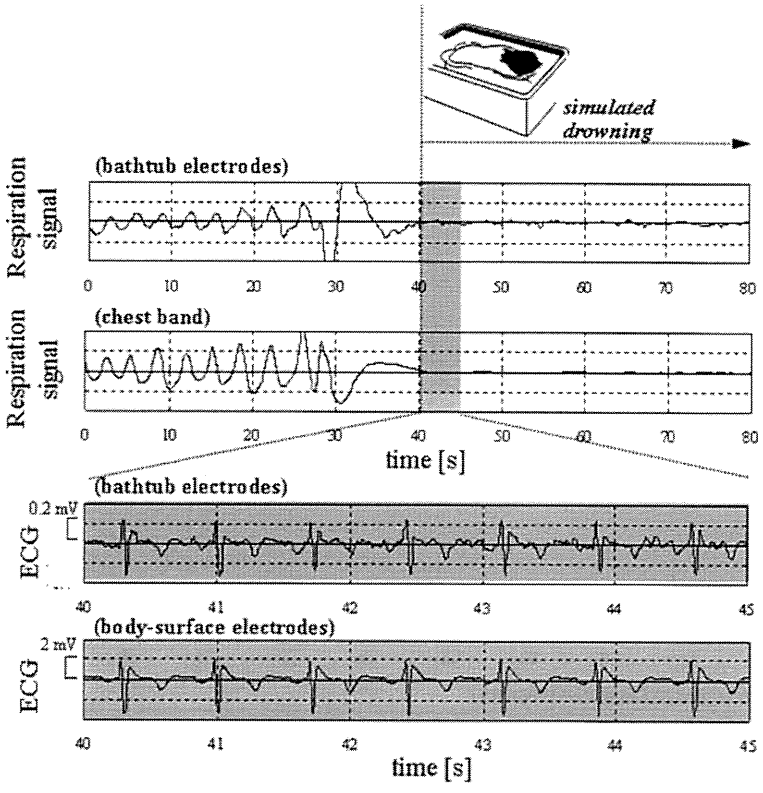

Fig. 11. Example of respiration signals (upper part) obtained by the bathtub electrodes (upper record) and a chest band (lower record) before and immediately after simulated drowning with the head bent forward in a healthy male subject (24 yrs). In the lower two records are shown ECG signals obtained by the bathtub electrodes (upper panel) and ECG electrodes directly attached to the subject's body surface (lower panel) during a part of drowning indicated by a shadow in the upper records.

and cardiac pulse signals obtained from the under-pillow sensor coincide well with those obtained from the body attachment sensors, and the period of apnea could also be definitely observed in respiration signals.

To investigate the applicability of this mode of health status monitoring in subjects with established clinical conditions, we have further developed the system to produce a new fully automated monitoring system, combining all the monitoring devices, and installed this in hospital rooms in Imizu City Hospital and Fujimoto Hayasuzu Hospital.[42] To date, we have found that the system is suitable for checking the health status of patients with chronic diseases, such as cardiac infarction and SAS, and that this monitoring appears superior to the conventional approach in the sense that it places less strain on the patient because there is no attachment of biological sensors. Further important data including the validity as well as clinical usefulness of the system have been reported.[42,43]

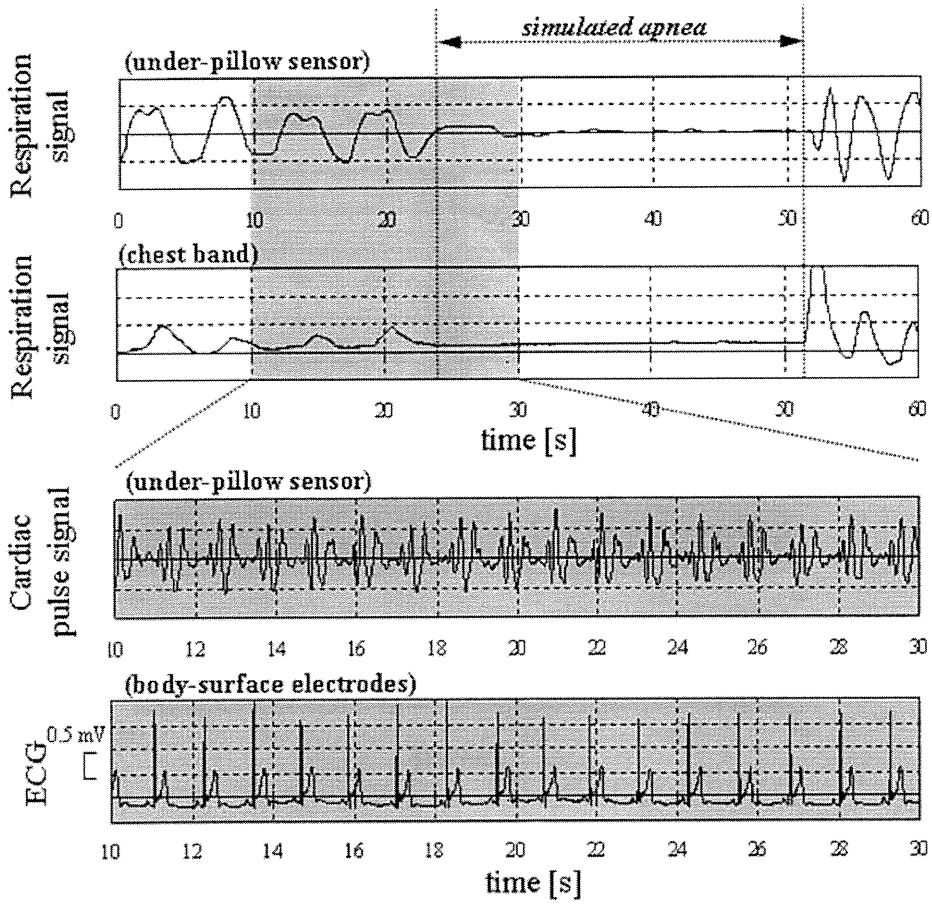

Fig. 12. Example of respiration signals (upper part) obtained by the under-pillow sensor (upper record) and a respiration chest band (lower record) before and immediately after a period of simulated apnea in a healthy male subject (25 yrs) in the supine position. In the lower part of this figure are shown cardiac pulse signal obtained by the under-pillow sensor (upper record) and ECG signal detected from the body surface electrodes (lower record) during a certain time indicated by a shadow in the upper part.

4. Summary and Future Developments

Recent developments and the present status of noninvasive bioinstrumentation for healthcare were briefly introduced in this review, including in particular the developments we have achieved. There are at present two research approaches in terms of monitoring techniques; one is ambulatory or wearable physiological monitoring and the other is nonconscious physiological monitoring. In light of the growth of the aging society, which has created what might be regarded as a longevity crisis, healthcare is one of the most serious and worldwide issues to address. Simple, convenient, and truly

ubiquitous healthcare monitoring in a fully automated as well as in a noninvasive manner could be the most useful and desirable.

The two research approaches described in this paper appear innovative and groundbreaking, particularly in the developments of instrumented garment systems and W-BAN with miniaturized sensors. It is optimistically anticipated that such easy-to-use devices could be made available at reasonable costs in the future, although there are still a number of challenging obstacles to be overcome, such as the rather conflicting requirements for size, wear comfort, operating procedures, precision, power management, and reliability.[1-6] Another problem is the fact that at present such devices only provide a limited range of physiological information derived from ECG, respiration, and simple motion signals. Given this situation, the ambulatory cardiovascular and activity monitoring devices described here would be even more suitable for practical use through further miniaturization, making them smaller and lighter with easier and more comfortable attachment to the body.

The approach described here for achieving nonconscious physiological monitoring at home would appear at the present time to be a near ideal solution, with good potential for practical use. The justification for this view is as follows. The individuals who might benefit from regular health assessment generally find using commercially available medical devices such as a BP monitor and a weighing scale quite troublesome or find it difficult to monitor their health conditions daily over a long period because these devices need the attachment of a biological sensor and manual operation for measurements. This inconvenience obstructs and deters long-term daily monitoring. In the nonconscious monitoring approach, however, the location of the systems in the toilet space, bathtub, and bed is considered to be very convenient and appropriate, because a subject at home uses these places everyday and reliable measurements can therefore be made within this stable and predictable situation.

It is therefore a fact that the nonconscious monitoring approach has made technological breakthroughs in achieving easier and more convenient acquisition of various physiological parameters at home. There are, however, still important practical issues to be solved in terms of interpretation methodology of a huge number of data and protection of personal information.

Taking a comparison of these ambulatory and nonconscious monitoring approaches into consideration, it is noted that, by addressing various issues mentioned above to complement both techniques, each approach will be practically available in a parallel way and the combination of these two will provide a much more useful and promising means.

In the so-called 'super-aging society,' these techniques could be relevant, contributing in many fields such as personal healthcare, medical care, and rehabilitation. To promote ubiquitous healthcare monitoring further, the establishment of appropriate social infrastructure that meets the needs of healthcare is urgently needed. Efforts to produce much more human-friendly sensing systems, where a number of practical problems still remain, are likely to be resolved through the considerable recent dramatic advances in microelectronic, micromechanical, information, and communication technologies.

Acknowledgements

The author wishes to thank Dr. Peter Rolfe, Director of Biohorizon Ltd. and Professor of Harbin Institute of Technology, for kind help in preparing the manuscript, Dr. Mitsuhiro Ogawa and Dr. Kosuke Motoi, Kanazawa University, for helpful discussion and assistance in the survey of current publications, Professor Shinobu Tanaka, Dr. Takehiro Yamakoshi, Kanazawa University, Dr. Hidetsugu Asanoi, Director of Imizu City Hospital, Dr. Toshiro Fujimoto, Administrative Director of Yokakai Association and Fujimoto Hayasuzu Hospital, Dr. Yuji Higashi and Mr. Tadahiko Yuji, Rehabilitation Center of Fujimoto Hayasuzu Hospital, for valuable discussion and considerable assistance during the progress of the research programs on instrumentation, data analysis, experimentation, and clinical evaluation. The studies were partly supported by the Knowledge-based Cluster Creation Project (Ishikawa High-tech Sensing Cluster, 2004–2009), and Grants-in-Aid for Scientific Research (No. 14208105, 2002–2004; No. 17300149, 2005–2007; No. 19700469, 2007–2008) from the Japan Ministry of Education, Culture, Sports, Science and Technology, and Strategic Information and Communications R&D Promotion Programme (SCOPE; No. 102305004, 2010) from the Japan Ministry of Internal Affairs and Communications, for which I wish to express my sincere appreciation.

References

1 J. Rantanen, J. Impiö, T. Karinsalo, M. Malmivaara, A. Reho, M. Tasanen and J. Vanhala: Personal and Ubiquitous Computing **6** (2002) 3.
2 L. Bourdon, S. Coli, G. Loriga, N. Taccini, B. Gros, A. Gemignani, D. Cianflone, F. Chapotot, A. Dittmar and R. Paradiso: Computers in Cardiology **32** (2005) 615.
3 R. Paradiso, G. Loriga, N. Taccini, A. Gemignani and B. Ghelarducci: J. Telecommun. Inf. Technol. **2** (2005) 105.
4 E. Jovanov, A. O. Lords, D. Raskovic, P. Cox, R. Adhami and F. Andrasik: IEEE Eng. Med. Biol. Magazine, May/June (2003) 49.
5 E. Jovanov, A. Milenkovic, C. Otto and P. C. Groen: J. NeuroEng. Rehabilitation **2** (2005) (http.//www.jneuroengrehab.com/content/2/1/6: Accessed on April 2010).
6 C. Otto, A. Milenkovic, C. Sanders and E. Jovanov: J. Mobile Multimedia **1** (2006) 307.
7 K. Yamakoshi: Non-Invasive Cardiovascular Hemodynamic Measurements, Sensors in Medicine and Health Care, eds. P. A. Öberg, T. Togawa, F. A. Spelman (Wiley-VCH Verlag GmbH & Co. KGaA, Weinheim, 2004) p. 107.
8 K. Motoi, S. Tanaka, Y. Kuwae, T. Yuji, Y. Higashi, T. Fujimoto and K. Yamakoshi: J. Robotics and Mechtronics **19** (2007) 656.
9 M. Ishijima and T. Togawa: Clin. Phys. Physiol. Meas. **10** (1989) 171.
10 M. Ishijima: Med. Biol. Eng. Comput. **35** (1997) 685.
11 Y. G. Lim, K. K. Kim and K. S. Park: IEEE Trans. Biomed. Eng. **54** (2007) 718.
12 P. Chow, G. Nagendra, J. Abisheganaden and Y. T. Wang: Physiol. Meas. **21** (2000) 345.
13 K. Watanabe, T. Watanabe, H. Watanabe, H. Ando, T. Ishikawa and K. Kobayashi: IEEE Trans. Biomed. Eng. **52** (2006) 2100.
14 K. Yamakoshi: Frontiers Med. Biol. Eng. **10** (2000) 139.
15 S. Tanaka, M. Nogawa and K. Yamakoshi: Proc. IEEE Eng. Med. Biol. 27th Annual Conf. Shanghai, CD-ROM (2005).

16 X. Zhu, W. Chen, T. Nemoto, Y. Kanemitsu, K. Kitamura, K. Yamakoshi and D. Wei: IEEE Trans. Biomed. Eng. **53** (2006) 2553.
17 K. Motoi, S. Kubota, A. Ikarashi, M. Nogawa, S. Tanaka, T. Nemoto and K. Yamakoshi: Proc. 29th Annual Conf. IEEE Engineering in Medicine and Biology Society (2007) 1826.
18 N. J. Holter: Science **134** (1961) 1214.
19 G. W. Mauck, C. R. Smith, L. A. Geddes and J. D. Bourland: J. Biomech. Eng. **102** (1980) 28.
20 K. Yamakoshi: J. Ambul. Monit. **4** (1991) 123.
21 K. Yamakoshi, A. Kawarada, A. Kamiya, H. Shimazu and H. Ito: Med. Biol. Eng. Comput. **23** (1985) 459.
22 S. Tanaka and K. Yamakoshi: Med. Biol. Eng. Comput. **34** (1996) 441.
23 K. Yamakoshi, M. Nakagawara and S. Tanaka: Biocybern. Biomed. Eng. **17** (1997) 181.
24 M. Nakagawara and K. Yamakoshi: Med. Biol. Eng. Comput. **38** (2000) 17.
25 K. Motoi, S. Tanaka, M. Nogawa and K. Yamakoshi: SICE Annual Conf. Proc. (2003) 563.
26 S. Tanaka, K. Yamakoshi and P. Rolfe: Med. Biol. Eng. Comput. **32** (1994) 357.
27 K. Motoi, Y. Higashi, Y. Kuwae, T. Yuji, S. Tanaka and Y. Yamakoshi: Proc. 27th Annual Conf. IEEE Eng. Med. Biol. CD-ROM (2005).
28 K. Motoi, K. Ikeda, Y. Kuwae, T. Yuji, Y. Higashi, M. Nogawa, S. Tanaka and Y. Yamakoshi: Proc. 28th Annual Conf. IEEE Eng. Med. Biol. Soc. CD-ROM (2006).
29 K. Yamakoshi, H. Shimazu and T. Togawa: IEEE Trans. Biomed. Eng. BME-**27** (1980) 150.
30 H. Ito, K. Yamakoshi and T. Togawa: J. Appl. Physiol. **40** (1976) 451.
31 A. Ikarashi, M. Nogawa, S. Tanaka and K. Yamakoshi: Proc. 29th Annual Conf. IEEE Eng. Med. Biol. Soc. (2007) 4580.
32 A. Hendry, W. Gilchrist, G. Duncan, A. L. Evans and D. C. Smith: Med. Biol. Eng. Comput. **28** (1990) 602.
33 S. Miyazaki: IEEE Trans. Biomed. Eng. **44** (1997) 753.
34 R. Williamson and B. J. Andrews: Med. Biol. Eng. Comput. **39** (2001) 1.
35 R. E. Mayagoitia, J. C. Lotters, P. H. Veltink and H. Hermens: Gait and Posture **16** (2002) 55.
36 M. Sekine, T. Tamura, M. Akay, T. Fujimoto, T. Togawa and Y. Fukui: IEEE Trans. Rehab. Eng. **10** (2002), 188.
37 B. Najafi, K. Aminian, A. Paraschiv-Ionescu, F. Loew, C. J. Bula and P. Robert: IEEE Trans. Biomed. Eng. **50** (2003) 711.
38 H. Dejnabadi, B. M. Jolles, E. Casanova, P. Fua and K. Aminian: IEEE Trans. Biomed. Eng. **53** (2006) 1385.
39 K. Yamakoshi, H. Shimazu, M. Shibata and A. Kamiya: Med. Biol. Eng. Comput. **20** (1982) 307 and 314.
40 K. Yamakoshi: Proc. 18th Annual Intern. Conf. IEEE Eng. Med. Biol. Soc. (1996) 10.
41 K. Yamakoshi: IEEE Rev. Biomed. Eng. **2** (2009) 2.
42 K. Motoi, M. Ogawa, H. Ueno, Y. Kuwae, A. Ikarashi, T. Yuji, Y. Higashi, S. Tanaka, T. Fujimoto, H. Asanoi and K. Yamakoshi: Proc. 31st Annual Intern. Conf. IEEE Eng. Med. Biol. Soc. (2009) 4323.
43 K. Motoi, A. Ikarashi, S. Tanaka, K. Yamakoshi. Ubiquitous Healthcare Monitoring for Daily Life, Distributed Diagnosis and Home Healthcare, eds. U. R. Acharya *et al.* (American Scientific Publishers, 2010) (in press).

About the Author

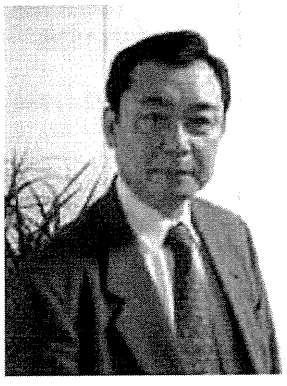

Ken-ichi Yamakoshi

Final affiliated college and degrees: He received his B. Sc and M.Sc degrees from Waseda University in 1970 and 1972, and D. Med. and D. Eng. degrees from Tokyo Medical and Dental University in 1979 and Waseda University, Tokyo, Japan in 1982, respectively.

Career summary: Professor Yamakoshi is a biomedical engineer with a career spanning about 40 years. He started as a Research Assistant at Tokyo Women's Medical College from 1972 to 1973, then as a Research Assistant at Tokyo Medical and Dental University from 1974 to 1980, an Associate Professor at Hokkaido University from 1980 to 1994, and has been a Professor at Kanazawa University since 1994. He is also currently a Visiting Professor at Dalian University, Dalian, China, Heilongjiang University, Harbin, China, and at Waseda University. Much of his research over this period has been concerned with noninvasive and/or ambulatory physiological measurement and instrumentation, nonconscious healthcare monitoring, human support systems, artificial organs, cardiovascular biomechanics and rehabilitation engineering. He has been an Associate Editor of the Institute of Electrical and Electronics Engineers (IEEE) Transactions on Biomedical Engineering and IEEE Transactions on Information Technology in BioMedicine, and an Area Editor of IEEE Reviews in Biomedical Engineering. He has also been the Director of two venture companies set up through research achievements.

Special field of study: Physiological measurement and instrumentation, healthcare science, cardiovascular and orthopedic biomechanics, rehabilitation engineering.

Society memberships: International Federation of Medical and Biological Engineering, IEEE Engineering in Medicine and Biology Society, Japanese Society for Medical and Biological Engineering, Japan Society of Mechanical Engineers, Society of Instrument and Control Engineers, Japan Association for Clinical Monitoring, and so on.

循環器内科，68(5)：496-498，2010

話　題

アルツハイマー病に用いられるドネペジルの抗心不全作用*

佐　藤　隆　幸**

Key Words : acetylcholine, heart failure, remodeling, vagus nerve, ventricular function

はじめに

われわれはこれまでに，迷走神経の電気刺激によって慢性心不全の進行が防止され，生命予後が改善される可能性を動物実験で明らかにしてきた[1]．近年では，イスラエルのBioControl Medical社によって植え込み型迷走神経刺激装置が開発され，臨床試験が行われている．研究の成功が大いに期待されるところである．

一方われわれは，迷走神経刺激が抗心不全作用を発揮する機序について分析するとともに[2)~4)]，既存の臨床薬剤の中で同様の機序を駆動する可能性のあるものを探索してきた．

塩酸ドネペジル(アリセプト®)はアルツハイマー病における認知症の進行を抑制する薬剤としてわが国で開発され，脳内のアセチルコリンエステラーゼ(AChE)を抑制することによって，その効果を発揮すると考えられている．われわれは最近，マウス心不全モデルを用いた研究によって，ドネペジルが抗心不全作用を有することを明らかにした[5]．

マウスの慢性心不全モデル

体重35g前後の雄マウスに腹部大動脈―下大静脈シャント術を行い，容量負荷型心不全モデルを作成した．心不全モデルの妥当性を術後4週で検討した．表1に示すように，4週目には心室拡張を伴った心不全が進行していると考えられた．覚醒下心拍数は偽手術群に比べ，むしろ減少していた．おそらく，著名な心房拡張と線維化によってもたらされたと考えられる．ランゲンドルフ灌流標本による圧容積関係の解析ではV_0の増加とE_{es}の低下が認められ，シャント術後4週目には心臓ポンプ機能の低下がもたらされていると考えられた．

ドネペジルの不全心に与える影響

腹部大動脈―下大静脈シャント術から4週後にマウスを無作為に2群に分け，無治療群とドネペジル治療群とした．治療群では飲水中にドネペジルを溶かし，1日用量がkg体重あたり5 mgになるようにした．用量設定は，ドネペジルを用いたマウスやラットの神経学的研究のプロトコールを参考に行った．4週間の治療後に血行動態を評価した．

表2に示すように，無治療群では心室拡張と心機能低下がさらに進展し，心臓リモデリングが進行している．一方ドネペジル治療群では，このような心不全増悪が有意に防止されている．心不全重症度の臨床マーカーのひとつである脳型ナトリウム利尿ペプチドの心室での発現も治療群では低下し，心不全の改善を示唆していると考えられる．

ドネペジルの慢性心不全の生命予後に与える影響

腹部大動脈―下大静脈シャント術から4週後にマウスを無作為に2群に分け，無治療群とド

* Anti-Alzheimer's drug, donepezil, improves survival after chronic heart failure in mice.

** Takayuki SATO, M.D., Ph.D.: 高知大学医学部循環制御学〔〒783-8505 南国市岡豊町小蓮〕; Department of Cardiovascular Control, Kochi Medical School, Nankoku 783-8505, JAPAN

表1　心不全モデルの特徴

		偽手術群	シャント術群
覚醒下での計測	・匹数	12	12
	・心拍数(beats/min)	700±13	643±9*
	・収縮期血圧(mmHg)	112±7	103±3
麻酔下での計測	・匹数	5	5
	・心拍数(beats/min)	480±53	470±24
	・左室拡張末期圧(mmHg)	3.71±0.33	8.05±1.02*
	・左室収縮ピーク圧(mmHg)	135.6±25.7	119.6±10.1*
	・dp/dt_{max}(mmHg/sec)	8,120±1,134	5,620±881*
灌流標本での計測	・匹数	7	7
	・V_0(μl)	1.2±0.2	2.2±0.3*
	・E_{es}(mmHg/μl)	1.96±0.16	1.32±0.04*
心重量の計測	・匹数	12	12
	・両心室重量(mg/g)	4.48±0.18	5.56±0.10*

dp/dt_{max}：左室圧の時間微分ピーク値，V_0：収縮期末圧容積関係における容積軸切片，E_{es}：収縮期末エラスタンス．値は平均±標準偏差．* $P<0.05$

表2　ドネペジル治療の不全心に与える影響

		無治療群	治療群
覚醒下での計測	・匹数	20	20
	・心拍数(beats/min)	573±11	643±11*
	・収縮期血圧(mmHg)	105±10	108±15
麻酔下での計測	・匹数	10	10
	・心拍数(beats/min)	522±51	519±42
	・左室拡張末期圧(mmHg)	14.9±0.8	10.2±1.6*
	・左室収縮ピーク圧(mmHg)	91.6±11.3	104.3±8.6*
	・dp/dt_{max}(mmHg/sec)	4,506±997	5,961±562*
灌流標本での計測	・匹数	10	10
	・V_0(μl)	5.1±0.4	3.1±0.3*
	・E_{es}(mmHg/μl)	0.96±0.09	1.47±0.05*
心重量の計測	・匹数	20	20
	・両心室重量(mg/g)	6.07±0.78	5.64±0.68*
左室でのBNP発現	・匹数	10	10
	・BNP mRNA(a.u.)	0.56±0.08	0.37±0.06*

dp/dt_{max}：左室圧の時間微分ピーク値，V_0：収縮期末圧容積関係における容積軸切片，E_{es}：収縮期末エラスタンス，BNP：脳型ナトリウム利尿ペプチド，a.u.：任意単位．値は平均±標準偏差．* $P<0.05$

ネペジル治療群とし，50日間の生存率を観察した．

図1にKaplan-Meier生存率曲線を示す．無治療群では50日の観察期間中に約半数が死亡したが，治療群では2割の死亡数であった．ドネペジルによって相対的死亡危険率がおおよそ6割減少した．

ドネペジルの抗心不全作用のメカニズム

ドネペジルの抗心不全作用として，当初β遮断薬のような徐脈作用を介する機序が想定されたが，表2に示すように，このような機序は否定的であった．そこで，新生仔心筋細胞培養系を用いてドネペジルの効果を検証した．その結果，ドネペジルは心筋細胞に作用して，hypoxia inducible factor-1α(HIF-1α)，vascular endothelial growth factor(VEGF)の発現を刺激すること，その作用がムスカリン受容体遮断薬，ニコチン受容体遮断薬では阻害されないことを見出した．

詳しい機序は不明であるが，ドネペジルが直接心筋細胞に作用してHIF-1αやVEGFなどの細胞生存因子の合成を刺激し，心筋細胞死を抑制す

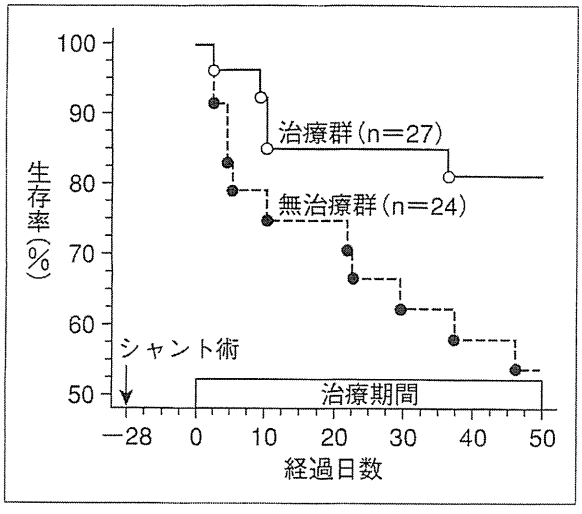

図1　ドネペジルの生存率に与える影響

ることによって抗心不全効果をもたらした可能性がある．これらの効果は，AChE阻害作用とは独立したものである可能性が高く，たいへん興味深い．

ドネペジルの心血管死に与える影響に関する臨床研究

これまでの動物実験の結果をふまえて，共同研究機関である米国Vanderbilt大学のSatoらがドネペジルの心血管死に与える影響について後ろ向き調査を行った[6]．アルツハイマー型認知症例でドネペジルを服用している例と服用していない例を中心に平均30か月の観察を行ったところ，服用群では心血管死のリスクが4割程度減少していることが明らかになった．多変量解析の結果でも，ドネペジル服用が独立したリスク要因であることが示された．しかし，比較した症例数がそれぞれ80例程度と少数であること，後ろ向き調査であることから，より信頼性の高い結果を得るために，より大規模な前向き調査が期待される．

おわりに

アルツハイマー病の認知障害の進行を防止する薬剤として幅広く使用されているドネペジルが，抗心不全効果や心血管死防止効果を発揮する可能性を示唆する知見が得られつつある．ごく最近では，ドネペジルが心筋細胞や血管内皮細胞に作用してアセチルコリン（ACh）の産生・放出を刺激し[7]，さらに，*de novo* AChのautocrine, paracrine的機序により，心筋細胞死を防止したり，血管新生を誘導する可能性も示唆されている[8]．今後，さらに研究が進めば，ドネペジルが慢性心不全や虚血性心疾患に対する治療薬の新機軸になる可能性がある．

文　献

1) Li M, Zheng C, Sato T, et al. Vagal nerve stimulation markedly improves long-term survival after chronic heart failure in rats. Circulation 2004 ; 109 : 120.
2) Ando M, Katare RG, Kakinuma Y, et al. Efferent vagal nerve stimulation protects heart against ischemia-induced arrhythmias by preserving connexin43 protein. Circulation 2005 ; 112 : 164.
3) Kakinuma Y, Ando M, Kuwabara M, et al. Acetylcholine from vagal stimulation protects cardiomyocytes against ischemia and hypoxia involving additive non-hypoxic induction of HIF-1 alpha. FEBS Lett 2005 ; 579 : 2111.
4) Katare RG, Ando M, Kakinuma Y, et al. Vagal stimulation prevents reperfusion injury through inhibition of opening of mitochondrial permeability transition pore independent of the bradycardiac effect. J Thorac Cardiovasc Surg 2009 ; 137 : 223.
5) Handa T, Katare RG, Kakinuma Y, et al. Anti-Alzheimer's drug, donepezil, markedly improves long-term survival after chronic heart failure in mice. J Card Fail 2009 ; 15 : 805.
6) Sato K, Urbano R, Yu C, et al. The effect of donepezil on cardiovascular mortality. Clin Pharmacol Ther 2010 ; 88 : 335.
7) Kakinuma Y, Akiyama T, Sato T. Cholinoceptive and cholinergic properties of cardiomyocytes involving an amplification mechanism for vagal efferent effects in sparsely innervated ventricular myocardium. FEBS J 2009 ; 276 : 5111.
8) Kakinuma Y, Furihata M, Akiyama T, et al. Donepezil, an acetylcholinesterase inhibitor against Alzheimer's dementia, promotes angiogenesis in an ischemic hindlimb model. J Mol Cell Cardiol 2010 ; 48 : 680.

Review

Am J Physiol Regul Integr Comp Physiol 300: R818–R826, 2011.
First published February 2, 2011; doi:10.1152/ajpregu.00426.2010.

Imbalance of central nitric oxide and reactive oxygen species in the regulation of sympathetic activity and neural mechanisms of hypertension

Yoshitaka Hirooka, Takuya Kishi, Koji Sakai, Akira Takeshita,† and Kenji Sunagawa

Department of Cardiovascular Medicine, Kyushu University Graduate School of Medical Sciences, Fukuoka, Japan

Submitted 29 June 2010; accepted in final form 29 January 2011

Hirooka Y, Kishi T, Sakai K, Takeshita A, Sunagawa K. Imbalance of central nitric oxide and reactive oxygen species in the regulation of sympathetic activity and neural mechanisms of hypertension. *Am J Physiol Regul Integr Comp Physiol* 300: R818–R826, 2011. First published February 2, 2011; doi:10.1152/ajpregu.00426.2010.— Nitric oxide (NO) and reactive oxygen species (ROS) play important roles in blood pressure regulation via the modulation of the autonomic nervous system, particularly in the central nervous system (CNS). In general, accumulating evidence suggests that NO inhibits, but ROS activates, the sympathetic nervous system. NO and ROS, however, interact with each other. Our consecutive studies and those of others strongly indicate that an imbalance between NO bioavailability and ROS generation in the CNS, including the brain stem, activates the sympathetic nervous system, and this mechanism is involved in the pathogenesis of neurogenic aspects of hypertension. In this review, we focus on the role of NO and ROS in the regulation of the sympathetic nervous system within the brain stem and subsequent cardiovascular control. Multiple mechanisms are proposed, including modulation of neurotransmitter release, inhibition of receptors, and alterations of intracellular signaling pathways. Together, the evidence indicates that an imbalance of NO and ROS in the CNS plays a pivotal role in the pathogenesis of hypertension.

blood pressure; sympathetic nervous system; central nervous system; nitric oxide; oxidative stress

ACTIVATION OF THE SYMPATHETIC nervous system is critically involved in the pathogenesis of hypertension, from initial occurrence to the development of target organ damage, such as heart failure, stroke, and renal failure (35, 36). The importance of the effects of the renin-angiotensin system on the sympathetic nervous system in the pathogenesis of hypertension is recently highlighted (30, 31). This is not surprising because both the autonomic nervous system and hormonal factors are the major regulators of blood pressure; therefore, abnormalities of either system are likely to be involved in the pathogenesis of essential hypertension (30, 31, 37). Esler (30) reported that the sympathetic nervous system is activated in ~50% of patients with hypertension, particularly in patients with essential hypertension. Central sympathetic outflow is determined by several important nuclei and their circuits in the central nervous system (CNS) (9, 81). These pathways involve many neurotransmitters and neuromodulators (16, 25, 38, 99). In particular, the brain stem circuitry is now considered crucial for the pathogenesis of hypertension, including both excitatory and inhibitory inputs from the supramedullary nuclei and the baroreceptors (16, 25, 38, 100, 115). In this review, we focus on the role of nitric oxide (NO) and reactive oxygen species (ROS) in the brain stem as factors constituting the neural mechanisms of hypertension. Because of the close relationship between NO and ROS, we discuss the individual roles of NO and ROS in the brain stem in central mechanisms of hypertension, and then the relationship between the two. Finally, we will discuss the possibility of targeting some cardiovascular drugs to improve the imbalance of NO and ROS.

NO in the Brain

NO is an important mediator of intracellular signaling in various tissues, including the CNS (32, 118, 119). NO acts via the second messenger cyclic GMP (32). Thus, soluble guanylate cyclase is its receptor. NO is synthesized from its precursor, L-arginine, by endogenous NO synthase (NOS). There are three NOS isoforms: constitutive enzymes, such as neuronal NOS (nNOS) and endothelial NOS (eNOS), and inducible enzymes such as inducible NOS (iNOS). A number of studies have demonstrated the localization of the nNOS, eNOS, and iNOS within the CNS using in situ hybridization and histochemical staining with NADPH-diaphorase or immunohistochemistry (8). nNOS is abundant in neurons. Considerable evidence indicates that NOS acts on central and peripheral sites throughout the autonomic nervous system, which controls the cardiovascular system, including the receptors and effectors of the baroreflex pathway (70, 95, 129).

Role of NO in the Brain Stem in Controlling Blood Pressure

Chronic administration of the NO synthesis inhibitor N^{ω}-nitro-L-arginine methyl ester (L-NAME) in drinking water induces a large increase in blood pressure in rats (29). Gangli-

† Deceased March 15, 2009.

Address for reprint requests and other correspondence: Y. Hirooka, Dept. of Cardiovascular Medicine, Kyushu Univ., Graduate School of Medical Sciences, 3-1-1 Maidashi, Higashi-ku, Fukuoka 812-8582, Japan (e-mail: hyoshi@cardiol.med.kyushu-u.ac.jp).

onic blockade elicits a greater fall in blood pressure in L-NAME-treated rats compared with controls, suggesting that the level of central sympathetic outflow in L-NAME-treated rats is greater than that in control rats. Microinjection of an ANG II type 1 (AT_1) receptor blocker (candesartan), but not that of an AT_2 receptor blocker (PD123319), into the nucleus tractus solitarius (NTS) elicits a greater decrease in blood pressure, heart rate, and renal sympathetic nerve activity (RSNA) in L-NAME-treated rats than in control rats. These results suggest that increased RSNA contributes to hypertension induced by chronic NOS inhibition and that activation of the renin-angiotensin system in the NTS is involved, at least in part, in the increased RSNA via AT_1 receptors (29). The rostral ventrolateral medulla (RVLM), the vasomotor center, is also activated in this model of hypertension, suggesting enhanced central sympathetic outflow (9). Pharmacological inhibition of NOS evoked by N^G-monomethyl-L-arginine (L-NMMA) or L-NAME also induces large increases in blood pressure that are partially sympathetically mediated in humans (109).

Immunohistochemical studies have revealed a rich distribution of nNOS in the NTS (8). Microinjection of L-NMMA into the NTS elicits an increase in blood pressure and RSNA, regardless of whether the baroreceptors are intact in anesthetized rabbits (39). The neurons in the NTS are activated by NO projecting to the caudal ventrolateral medulla, thereby activating the inhibitory neurons in the caudal ventrolateral medulla, which project to the RVLM, and may ultimately result in decreased sympathetic nerve activity (SNA). Single-unit extracellular recordings of NTS neurons in rat brain stem slices revealed that L-arginine increases neuronal activity dose-dependently, but D-arginine does not (80, 116). L-NMMA blocks the L-arginine-induced increases in the neuronal activity. Sodium nitroprusside, an NO donor, also increases neuronal activity. Consistent with the findings from the in vivo studies (39), these results suggest that NO increases the neuronal activity in the NTS through an increase in cyclic GMP. It has been proposed that NO acts in an ultrashort feedback loop, in which the release of L-glutamate activates nNOS and subsequently the production of NO (32). The NO, in turn, diffuses to presynaptic terminals, where it modulates the release of L-glutamate in response to neuronal activation. Studies using in vivo microdialysis demonstrated that activation of NMDA receptors in the NTS induces the release of NO, and NMDA-induced NO production stimulates L-glutamate release (74, 75, 82). In addition, this mechanism is involved in the depressor and bradycardic responses evoked by NMDA receptor activation in anesthetized rats (82). To determine the effects of increased NO production in the NTS for much longer periods on blood pressure, heart rate, and urinary norepinephrine excretion, we developed an in vivo technique for eNOS gene transfer into the NTS of rats (43, 44, 46, 107). In this study, the successful transfer of the eNOS gene into the NTS was confirmed by several methods, including immunohistochemistry, Western blot analysis, and nitrite/nitrate concentration measurements (107). Changes in blood pressure and heart rate were observed using a radio-telemetry system. It is important to note that we used eNOS instead of nNOS, which is normally abundant in the CNS, because the purpose of the study was to increase NO production from constitutively expressed NOS. The results indicated that NO in the NTS exerts an inhibitory effect on SNA in vivo.

Compared to studies of the NTS, studies of the RVLM in both acute and anesthetized models have produced more conflicting results (42, 53, 66, 81, 112, 120, 131). Therefore, we applied the technique described above to studies of the RVLM (57, 58). In those studies, blood pressure, heart rate, and urinary norepinephrine excretion were decreased after eNOS gene transfer. Microinjection of either L-NMMA or bicuculine, a GABA receptor antagonist, into the RVLM after eNOS gene transfer increased blood pressure to greater levels in the eNOS gene transfer group compared with the mock gene transfer control group. GABA levels in the RVLM after the eNOS gene transfer measured by in vivo microdialysis were also increased in the eNOS gene transfer group. These results indicate that the increased NO production evoked by the overexpression of eNOS in the bilateral RVLM decreases blood pressure, heart rate, and SNA in awake rats. Furthermore, these responses are mediated by an increased release of GABA in the RVLM. These studies provided convincing evidence that chronic changes in neurotransmitters/neuromodulators in the RVLM have a sustained impact on blood pressure in awake animals.

There is no clear explanation for the different modulatory effects of NO on neurons between the NTS and RVLM. NO increases both excitatory and inhibitory amino acids in the RVLM (43, 57). NO has also been shown to increase both L-glutamate and GABA in the paraventricular nucleus of hypothalamus (49). Microinjection of kynurenic acid into the RVLM, however, did not alter blood pressure after eNOS gene transfer, although microinjection of bicuculline into the RVLM augmented the increase in blood pressure (57). Therefore, we consider that GABAergic inhibition of the RVLM neurons might be more powerful than the glutamatergic activation in the resting condition (43, 57). In contrast, the glutamatergic input into the NTS neurons might be more powerful than the GABAergic input. In the NTS, there are close anatomic connections between nNOS and glutamatergic receptors (75). Furthermore, increases in NO induce L-glutamate release and microinfusion of NMDA and AMPA increase NO levels, suggesting that there are facilitatory interactions between L-glutamate and NO (27, 74, 82), although there are no studies measuring GABA levels induced by NO in the NTS. Furthermore, higher concentrations of NO are required to directly engage GABAergic inhibition, while lower concentrations of NO might be important for glutamatergic transmission in the NTS (125). Thus, it is still difficult and complicated to explain the physiological response induced by NO in the NTS (119). With regard to the action of NO on neuronal activity, NO induces both excitatory and inhibitory postsynaptic currents that likely depend on the neuron examined (6, 7, 126, 127).

Effects of NO in the Brain System in Experimental Models of Hypertension

Neurogenic mechanisms are dominant in the pathogenesis of essential hypertension in ~50% of patients (30). Spontaneously hypertensive rats (SHR) or stroke-prone SHR (SHRSP) exhibit increased RSNA during the development of hypertension, and blood pressure and RSNA are positively correlated (52, 79). The L-arginine-NO pathway is disrupted in SHR and SHRSP. The depressor response to an intracerebroventricular injection of an NO donor is greater in SHRSP than in normo-

tensive control rats, whereas the pressor response to intracerebroventricular injection of L-NAME is smaller (13). Semiquantitative RT-PCRs and in situ hybridization in SHR and Wistar-Kyoto (WKY) rats at 4 (prehypertensive) and 14 (established hypertension) wk of age (101) indicate that eNOS mRNA expression changes with the development of hypertension. Although there are no differences between the groups at 4 wk of age, nNOS gene expression increases in the hypothalamus, dorsal medulla, and caudal ventrolateral medulla of SHR compared with WKY rats at 14 wk of age. In the RVLM, there are no differences between the groups. In the SHRSP, there are also no differences in nNOS expression levels in the RVLM compared with WKY rats (101). A recent study demonstrated that NOS activity, measured by the ability of tissue homogenate to convert [^{3}H]L-arginine to [^{3}H]L-citrulline in a calcium- and NADPH-dependent manner, is impaired in the cerebral cortex and brain stem of prehypertensive SHR (104). In contrast, NOS activity is increased in the hypothalamus and brain stem in SHR rats with established hypertension compared with WKY rats (104). Thus, attenuated NOS activity in the cortex and brain stem of prehypertensive SHR might play a role in the pathogenesis of hypertension, and the up-regulated NOS activity in the hypothalamus and brain stem of SHR with established hypertension might serve to compensate for the hypertension. The expression of iNOS mRNA and protein is under the limits of detection in the hypothalamus of both WKY rats and SHR (40). Decreased NOS activity measured by the nitrite and nitrate contents was also demonstrated in the hypothalamus of SHR (1). In hypertensive SHRSP, nNOS protein expression levels in the hypothalamus and brain stem were enhanced compared with those in WKY (59). In a renovascular hypertensive rat model, mRNA expression levels of nNOS and soluble guanylate cyclase genes are reduced in the hypothalamus but not in the dorsal medulla (69). Together, these results suggest that the L-arginine-NO pathway is impaired in hypertensive rats, including SHR, possibly because of a posttranscriptional abnormality (70). Overexpression of eNOS in the NTS results in a greater depressor response in SHR than in WKY rats in the awake state (44). In that study, eNOS was used instead of nNOS to increase NO production locally in the NTS. Findings from another study suggest that the depressed NO modulation is consistent with the lower NOS activity in the dorsal brain stem (103). Therefore, the abnormality in the L-arginine-NO pathway in the NTS might be involved in the maintenance of hypertension of SHR. A recent study by Waki et al. (121) demonstrated that endogenous eNOS activity in the NTS plays a major role in determining the blood pressure set point in SHR and contributes to maintaining high arterial blood pressure in this model, suggesting the possible involvement of neurovascular coupling (96). In the RVLM of SHRSP, overexpression of eNOS elicits greater depressor and sympathoinhibitory responses than in WKY (58). Furthermore, the increase in NO production evoked by the overexpression of eNOS in the RVLM enhances the inhibitory action of GABA on the RVLM neurons (58). The results indicate that NO dysfunction and the resulting disinhibition of the RVLM contribute to increase RSNA in SHRSP.

Effects of NO in the Brain Stem on Baroreflex Function

As described earlier, NO activity in the NTS and RVLM influences cardiovascular regulation. We examined the role of endogenous NO in the brain stem in the rapid central adaptation of baroreflex control of RSNA in anesthetized rabbits (41). Bilateral carotid sinuses were isolated, and a stepwise increase in pressure was applied to the carotid sinuses, while arterial pressure and RSNA were recorded. The procedure was performed after intracisternal injection of L-NAME, D-NAME, L-arginine, or the vehicle solution. L-NAME enhances the rapid adaptation of the arterial baroreflex control of renal sympathetic nerve activity in rabbits (41). Transmission of arterial baroreflex signals depends on NO (27, 118). It was reported that the baroreceptor reflex gain in awake animals was increased by NO in the bradycardic component, although in these studies NOS inhibitors were administered systemically to examine the role of NO on baroreflex function (78, 87). Furthermore, overexpression of eNOS in the RVLM improves impaired baroreflex control of heart rate in SHRSP (60).

In summary, NO in the brain stem, particularly in the NTS and RVLM, has a sympathoinhibitory function, thereby reducing blood pressure. NO in the brain stem also facilitates the baroreflex function. The sympathoinhibitory effects of NO are impaired in animal models of hypertension, and supplementation of NO in the brain stem in hypertensive rats attenuates the abnormality, thereby decreasing blood pressure. The facilitory release of neurotransmitters induced by NO might be involved in the synaptic transmission mechanism.

ROS in the Brain

Substantial evidence also indicates that increased oxidative stress is involved in the pathogenesis of hypertension (12, 47, 48, 94, 99). ROS, such as superoxide anions and hydroxyl radicals, increase oxidative stress. There are several sources of ROS generation, such as NADPH oxidase, xanthine oxidase, mitochondria, and NOS uncoupling (12, 47, 48, 94, 99). On the other hand, reduction of antioxidant enzymes, such as superoxide dismutases (SOD), also induces an increase in oxidative stress (47, 48, 99). Although the role of ROS in the regulation of blood pressure in the normotensive state is not clear, increased ROS generation in the brain stem contributes to neural mechanisms of hypertension (47, 48). For example, although there is evidence of an increase in oxidative stress in the vasculature in hypertension, we showed, for the first time, that increased ROS in the RVLM contributes to SNA, leading to the neural mechanisms of hypertension in SHRSP (61). Zimmerman et al. (133) demonstrated that hypertension caused by low doses of circulating ANG II depends on the production of superoxide in the circumventricular organs (133). It was demonstrated that physiological responses to brain ANG II involve ROS production (15, 132, 133). Considering the importance of the brain ANG II system (2, 10, 26, 28, 83, 85, 86, 108), ROS play an important role in the neural regulation of blood pressure because ROS production largely depends on AT_1 receptor stimulation (47, 48, 99).

Role of ROS in Neural Mechanisms of Hypertension

As described earlier, on the basis of results demonstrating that microinjection of Tempol or overexpression of manga-

nese-superoxide dismutase in the RVLM markedly decreases blood pressure in SHRSP, but not in WKY, increased oxidative stress in the RVLM contributes to the neural mechanisms of hypertension in SHRSP (61). Oxidative stress levels in the RVLM were determined by measuring thiobarbituric acid-reactive substances (TBARS) levels and electron spin resonance (ESR) spectroscopy with a spin trapping technique (47, 48, 61). In SHR, oxidative stress in the RVLM plays an important role in hypertension via activation of the sympathetic nervous system (19, 66, 106, 117). An increase in oxidative stress in the RVLM also contributes to hypertension via activation of the sympathetic nervous system in rats with renovascular hypertension (two-kidney one-clip hypertensive model) (92). This model is an ANG II-dependent model of hypertension. Therefore, it is conceivable that ANG II increases oxidative stress by acting both centrally and peripherally, thereby activating the sympathetic nervous system and leading to hypertension as one of the hypertensive mechanisms in this model. AT_1 receptor expression levels in the RVLM and the paraventricular nucleus of the hypothalamus are enhanced in this rat renovascular model of hypertension (93). Interestingly, NADPH oxidase activity is increased, but Cu/Zn-SOD expression in the RVLM is unchanged. In a subsequent study, the authors showed that oxidative stress increased in both the RVLM and paraventricular nucleus, as well as systemically in this hypertensive model (93). These results suggest that systemic activation of the renin-angiotensin system activates AT_1 receptors in the brain, including the RVLM and paraventricular nucleus, thereby increasing SNA, leading to hypertension, as one of the mechanisms.

Sources of ROS Generation in the Brain Stem

NADPH oxidase is a major source of ROS in hypertension (71, 72) and has a critical role in generating ROS in the brain (5, 14, 51, 90, 122, 134). ANG II is upstream of NADPH oxidase activation, which requires Rac1 (48, 90, 122, 134). NADPH oxidase-derived ROS are involved in the effects of ANG II on Ca^{2+} influx in the NTS neurons receiving vagal afferents (122). Importantly, the essential subunit of NADPH oxidase, gp91phox, is present in somatodendritic and axonal profiles containing AT_1 receptors (122). The potentiation of Ca^{2+} currents indicates that ANG II increases neuronal excitability and spontaneous activity in some neurons (135). ANG II failed to increase ROS production or to potentiate L-type Ca^{2+} currents in the dorsomedial portion of the NTS neurons of mice lacking Nox2 (123). Thus, the excitatory actions of ANG II in the NTS neurons are caused, at least, in part, by the activation of L-type Ca^{2+} channels. It should be noted that ANG II-induced inhibition of neuronal delayed rectifying potassium current (I_{KV}) is mediated by ROS in primary neurons isolated from the hypothalamus and brain stem, because both NAD(P)H oxidase inhibition and Tempol prevented the ANG II inhibition of I_{KV} (113).

Mitochondria are another source of ROS generation in the brain. Chan et al. (21) examined the role of the mitochondrial electron transport chain in the RVLM of SHR and found that mitochondrial electron transport chain dysfunction in the RVLM of SHR depressed complex I or III activity and reduced the electron transport capacity (ETC) between complexes I and III or II and III (21). Interestingly, microinjection of coenzyme Q_{10} into the RVLM of SHR reversed the depressed ETC activity and enhanced superoxide generation. In addition, microinjection of antisense oligonucleotide against the p22phox subunit of NADPH oxidase into the RVLM reduced the enhanced ROS production in SHR (21). It is also important to note that microinjection of coenzyme Q_{10} into the RVLM of SHR decreases blood pressure (21). These results suggest that impairment of mitochondrial ETC complexes contributes to chronic oxidative stress in the RVLM of SHR, leading to enhanced central sympathetic drive and hypertension (21, 136). Consistent with their observation, we also found that ANG II induced the mitochondria-derived ROS production via activation of NADPH oxidase, although we did not find differences in the mitochondrial respiratory complexes between SHRSP and WKY (91), thus suggesting a feedforward system for ROS generation (21, 91, 136) (Fig. 1). Mitochondrial produced superoxide mediates the ANG II inhibition of I_{KV} (128). Recently, Chan et al. (22) suggested that transcriptional upregulation of mitochondrial uncoupling protein 2 (UCP2) in response to an increase in superoxide plays an active role in the feedback regulation of ROS production in the RVLM (22). Furthermore, oral treatment with rosiglitazone enhances a central antihypertensive effect via an upregulation of peroxisome proliferator-activated receptor-γ (PPAR-γ) and reduced oxidative stress in the RVLM of SHR (23). Stimulation of PPAR-γ results in the upregulation of UCP2, thereby reducing oxidative stress. The dose of rosiglitazone used in that study,

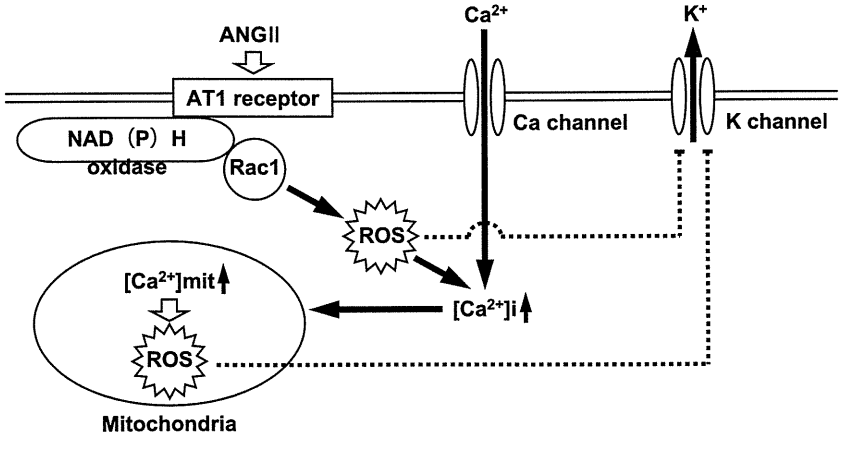

Fig. 1. A suggested scheme demonstrating that ANG II stimulation increases reactive oxygen species (ROS) generation via NAD(P)H oxidase and related mechanisms. [Modified from Nozoe et al. (91).]